



A VARIABLE DAMPING TUNED ABSORBER WITH ELECTRO-RHEOLOGICAL FLUID FOR TRANSIENT RESONANCE OF LIGHT STRUCTURES

T. D. TRUONG AND S. E. SEMERCIGIL

*School of the Built Environment (Mechanical Engineering), Victoria University of Technology,
Footscray Campus, P.O. Box 14428, MCMC Melbourne, Victoria 8001, Australia.
E-mail: eren@dingo.vu.edu.au*

(Received 13 August 1999, and in final form 26 November 1999)

Electro-rheological (ER) fluids can change from a liquid state into a solid-like gel under electrical potential. This change takes place within milliseconds and it is reversible once the electrical potential is removed. The proposed design in this investigation employs the unique characteristics of ER fluids to vary the damping of a tuned absorber. Numerical predictions from a simple model, and corresponding experimental observations are presented. ER fluids hold great promise in vibration control applications.

© 2001 Academic Press

1. INTRODUCTION

Tuned vibration absorbers are simple and effective passive vibration control devices for lightly damped resonance structures. A simple system including a tuned absorber is shown in Figure 1(a) under the effect of a sinusoidal excitation “ $F_0 \sin \omega t$ ”. The primary structure to be controlled has a mass m_1 , viscous damping coefficient c_1 and stiffness k_1 , where as m_2 , c_2 and k_2 represent the corresponding parameters of the tuned absorber. Vibration absorber is tuned by ignoring the damping in the system and by usually setting

$$(k_1/m_1)^{1/2} = (k_2/m_2)^{1/2},$$

where each side of the equality represents the undamped resonance frequency of the structure (ω_1) and the absorber alone (ω_2) respectively [1, 2]. This simple equality ensures that the absorber is at resonance at the most critical frequency (at ω_1 or ω_2) of the structure to be controlled. In resonance, the absorber uses all the available energy in the system providing ideal control for the primary structure. The absorber which undergoes quite violent oscillations is considered to be expendable. It may also be shown readily that, at the tuning frequency, the force of the absorber’s spring is of the same amplitude but of opposite sign with that of the external force $F_0 \sin \omega_2$.

In Figure 1(b), the steady state displacement amplitude of the undamped ($c_1 = 0$) primary structure, X_1 , is shown for different frequencies of the excitation $F_0 \sin \omega t$. The horizontal axis represents the non-dimensional frequency, ω/ω_1 , where ω_1 is the undamped resonance frequency. Results in Figure 1(b) are for $m_2/m_1 = 0.10$ and for three different critical damping ratios ($\zeta = c_2/2(k_2 m_2)^{1/2}$) of the absorber of 0, 0.05 and 0.20. When the primary structure is excited at the tuning frequency ($\omega = \omega_1$), perfect control effect is possible with an undamped absorber ($\zeta = 0$). This tuning may be very important practically if the primary

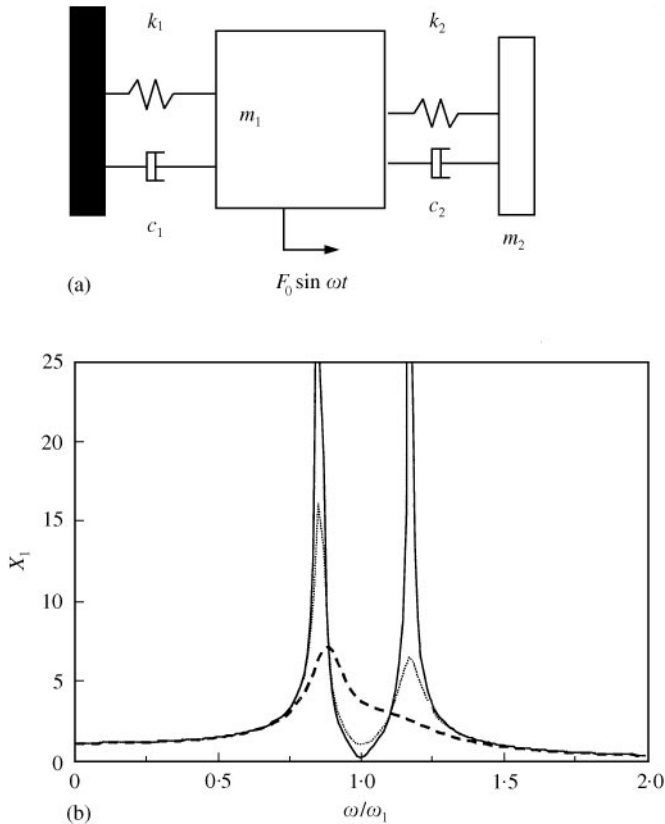


Figure 1. A simple mechanical oscillator with a tuned absorber; (b) steady state response of the primary structure for different excitation frequencies. ζ is the critical damping ratio of the absorber: ---, $\zeta = 0.20$; \cdots , $\zeta = 0.05$; —, $\zeta = 0$.

structure represents a machine which is designed to operate constantly at this particular tuning frequency.

One significant consequence of adding a tuned absorber to the primary system, is to introduce an additional resonance frequency at a frequency somewhat lower than the original resonance frequency. For $m_2/m_1 = 0.10$, the new resonance is approximately at $\omega = 0.8\omega_1$. The problem now is that as the machine is started from rest, before its steady operating frequency is reached at ω_1 , a resonance has to be traversed at about $0.8\omega_1$. Accelerating to the steady state frequency quickly would certainly alleviate this transient resonance problem. However, in order to provide a quick acceleration, the driver of the primary system should have enough reserve power. The driver would not normally need this reserve power at the steady speed, forcing the design to be a wasteful overdesign in order to avoid the transient resonance.

Including some damping in the tuned absorber reduces the transient resonance amplitudes significantly as shown in Figure 1(b) for the cases with ζ of 0.05 and 0.20. The problem this time, however, as the transient resonance amplitudes are reduced, the tuning effect is partially lost in the steady state. At the operating frequency, a damped tuned absorber is worse off than the undamped one depending upon the level of damping in it.

An ideal absorber would be the one to have the characteristics of a damped tuned absorber as the first resonance frequency is traversed, and those of the undamped one once the steady state operating frequency is reached. An electro-rheological fluid is used in this

study as the working fluid of a sloshing absorber. The unique feature, of changing phase between fluid and solid under applied electrical potential, of this particular fluid is then employed to manipulate the level of damping in the tuned absorber. Next, a brief description of sloshing absorbers and electro-rheological fluids is given with the suggested configuration for a variable damping tuned absorber. A simple numerical model is discussed to predict the performance. Finally, experimental observations are presented to support the assertions.

2. SLOSHING ABSORBER WITH AN ELECTRO-RHEOLOGICAL FLUID

Sloshing is the low-frequency oscillation of liquids in a container. In most cases, presence of sloshing is detrimental such as that in transportation of liquid cargo. Hence, effort required to suppress sloshing to enhance the integrity of the related application [3–5]. In contrast to the suppression, intentionally induced sloshing of a liquid may be exploited in a similar fashion to that of a tuned absorber. Instead of a mechanical oscillator, such an absorber utilizes the sloshing of a liquid to provide the required force opposition to achieve the control of a primary structure. The control force is the fluctuating pressure force on the sides of the container. Earlier work suggested promising designs for an effective sloshing absorber [6].

In a sloshing absorber, energy dissipation is the result of the shearing of the fluid as velocity gradients are developed within the flow. This dissipation also depends upon the viscosity of the liquid. A schematic representation of a sloshing absorber is shown in Figure 2 attached on the same primary structure as in Figure 1(a). An electro-rheological fluid is used in this study to provide a varying “apparent” viscosity to lead to a varying energy dissipation characteristics of a sloshing absorber.

Electro-rheology (ER) is the phenomenon in which the rheology of the fluid is manipulated by the imposition of electric fields. ER fluids are Newtonian in the absence of an electric field. However, when the electric field is raised to a high enough strength (in the order of several kV over distances of a few mm), ER fluid begins to assume the character of a solid-like gel and can be subjected to shear stresses [7, 8]. The phase change takes place over milliseconds, and it is completely reversible.

ER fluids are generally colloidal suspensions of fine semi-conducting polymer particles in dielectric base oil. Some examples of these semiconducting particles are cornstarch grain, cellulose, silica-gel or alumina powder whose particle sizes range from nano to micrometers. In the absence of electric potential, particles are dispersed in the suspension oil as shown in

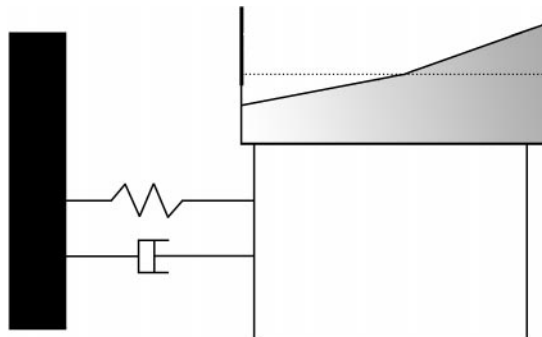


Figure 2. Sloshing absorber attached on the primary structure to be controlled.

Figure 3(a). When the electric field is applied, the particles in the fluid are polarised to form chains to link the electrodes, as shown in Figure 3(b). The formation of chains results in an effective enhancement of the “apparent” viscosity of the fluid to change it into a solid-like gel. Increased electric potential leads to higher shear strength [7,9,10].

As mentioned in the previous section, an ER fluid is suggested as the working fluid of a sloshing absorber to provide variable damping for a tuned absorber. When there is no

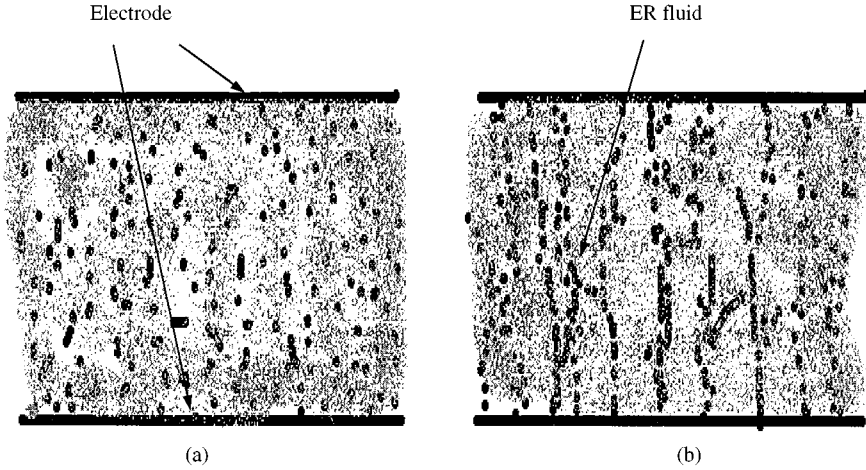


Figure 3. Schematic representation of an ER fluid (a) without and (b) with an electric potential across the electrodes.

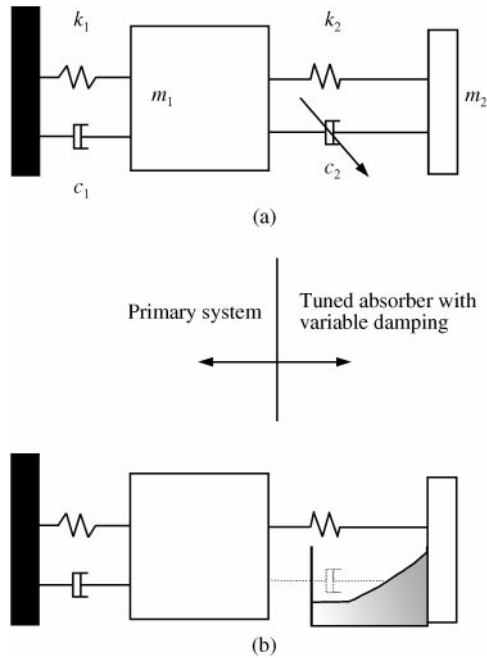


Figure 4. (a) Tuned absorber with variable damping and (b) sloshing absorber with ER fluid to provide variable damping.

voltage applied on the fluid, it is free to slosh and dissipate energy. Once the required voltage is applied, the phase of the liquid is transformed to that of a solid. In its transformed phase, it is no longer able to slosh to dissipate energy. The two very different energy dissipation characteristics may, therefore, be used to provide variable damping for the tuned absorber. As the frequency of excitation builds up to the steady state, the ER fluid is allowed to dissipate energy with no voltage applied across it. Once the steady state is reached, energy dissipation in the liquid can be "switched off" by solidifying the ER fluid. The suggested configuration is shown in Figure 4.

3. ENERGY DISSIPATION WITH SLOSHING ER FLUID

A simple experimental set-up is shown in Figure 5(a) to measure the amount of damping possible with a sloshing ER fluid. The structure consists of a light rigid plate suspended over four thin aluminium strips cantilevered from a fixed base. The container of the sloshing absorber is mounted on the rigid plate. The 100 mm nominal width of a square plastic food storage container is divided into five equal compartments with six aluminium electrodes of 0.5 mm thickness. Hence, 100 mm length of the sloshing wave is maintained for each compartment. Corn starch, of 40% volume fraction, dissolved in commonly available "light" paraffin oil is used as the ER fluid. Approximately 25 mm depth produced a fundamental sloshing frequency of 2.7 Hz. The fundamental frequency of the structure is also 2.7 Hz when the ER fluid is solidified. This experimental set-up is also used as the tuned absorber to control the primary structure to be described in Section 5. Structural parameters are summarized in Table 1.

Free decay of the simple oscillator was observed after giving it a predetermined initial displacement. The displacement history of the structure was sensed with a non-contact laser transducer and amplified (items 1 and 2) before it was recorded in a personal computer. Voltage for the ER fluid was provided by a high-voltage source (item 4) connected to the six aluminium electrodes in the plastic container. Only two electrodes are shown in the figure for clarity.

Two typical displacement histories are shown in Figure 5(b) and 5(c). In these figures, the oscillator is released from an initial displacement around 2.6 s. Of importance is the time-varying characteristics of energy dissipation. At the start, when there is a large amplitude sloshing wave, the equivalent viscous damping coefficient (ζ) could be measured to be as large as 0.20, whereas after about three peaks, the damping ratio assumes a value of about 0.05 and remains approximately constant. This trend is not surprising, considering that sloshing is a non-linear phenomenon, and a large amplitude sloshing wave imposes a more significant shearing action in the flow than that of a smaller wave.

A maximum of 5 kV was possible with the available voltage source which gave 0.25 kV/mm between the electrodes of the container shown in Figure 5(a). This electric potential is significantly lower than what is reported in the literature to form strong particle chains. However, the purpose here was to simply prevent sloshing rather than making a high-strength solid-like gel, 0.25 kV/mm was certainly observed to be sufficient for this purpose. As given in Table 1, damping ratio of the oscillator was measured to be around 0.02 with the full voltage when the ER fluid was solidified to act as an added mass.

4. NUMERICAL PREDICTIONS

A numerical study was conducted to predict benefits of varying the damping coefficient of the tuned absorber in Figure 1(a) as the frequency of excitation traversed from rest to the

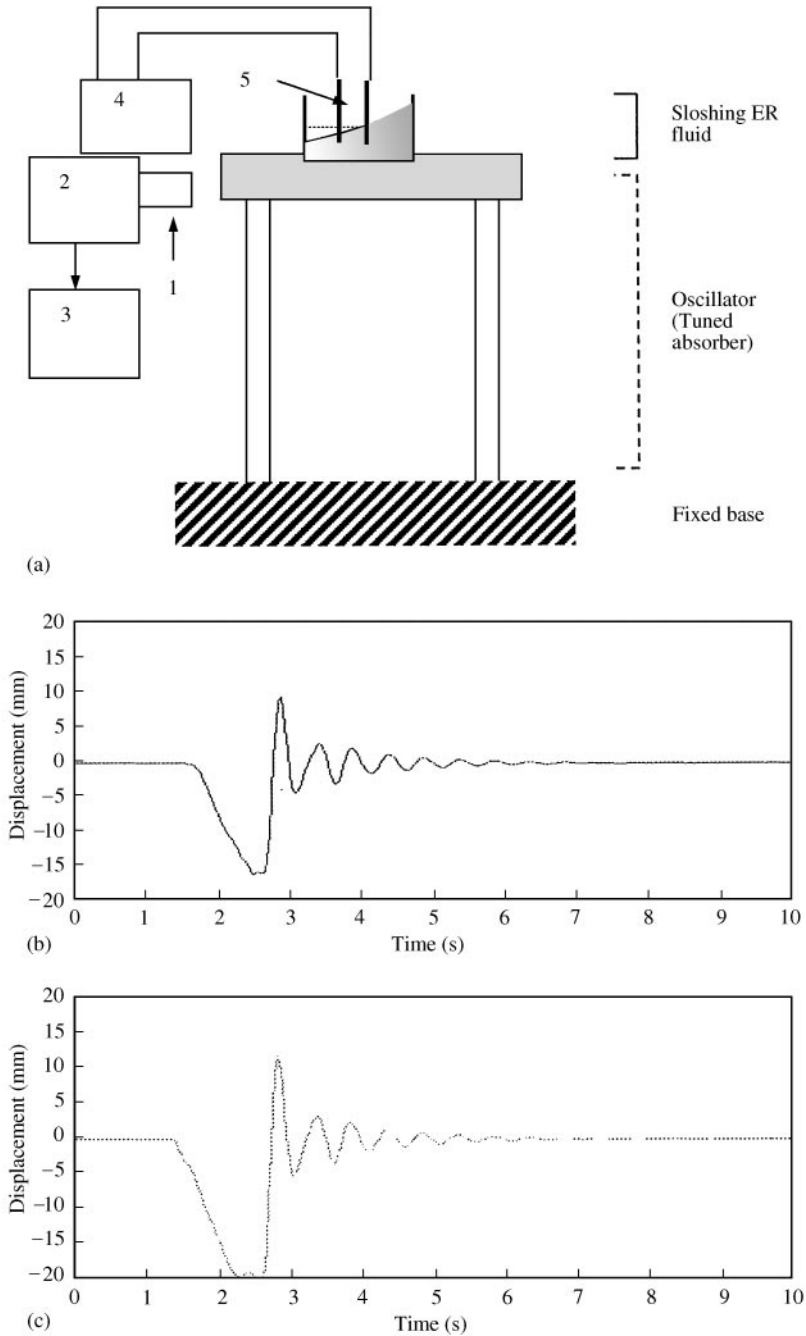


Figure 5. (a) Experimental set-up, (b) and (c) typical decay histories of the structure with no voltage. 1, KEYENCE LB-12 Laser transducer, 2, KEYENCE LB-72 amplifier; 3, computer with data acquisition and speed controller, 4, FLUKE 408B high-voltage source; 5, electrodes (0.5 mm thick aluminium).

tuning frequency. Differential equations of motion for this two-degree-of-freedom (d.o.f.) system are

$$m_1 \ddot{x}_1 + (c_1 + c_2) \dot{x}_1 - c_2 \dot{x}_2 + (k_1 + k_2)x_1 - k_2 x_2 = F(t) \tag{1}$$

TABLE 1

Structural parameters of the experimental set-up when each component is tested alone

| | Fundamental freq. (± 0.1 Hz) | Mass (± 0.01 kg) | Equivalent viscous damping ratio |
|-------------------------|--------------------------------------|--------------------------|--|
| Primary structure | 3.0 | 4.00 | 0.0075 ± 0.0005 |
| Sloshing container | 2.7 | 0.30 | — |
| Absorber with container | 2.7 | 0.40 | 0.020 ± 0.005 (at 0.25 kV/mm) $0.200/0.005 \pm 0.01$ (at 0 kV/mm) |

and

$$m_2 \ddot{x}_2 + c_2 \dot{x}_2 - c_2 \dot{x}_1 + k_2 x_2 - k_2 x_1 = 0 \quad (2)$$

In these equations, co-ordinates $x_1(t)$ and $x_2(t)$ represents the absolute displacement of m_1 and m_2 respectively. An overdot represents differentiation with respect to time. The numerical procedure consisted of preparing a program within the Matlab [11] environment to numerically integrate the coupled equations of motion using a fourth order Runge–Kutta scheme.

The external force in Figure 1(a) was specified to be $F(t) = (C\omega^2) \sin \omega t$ to represent a rotating unbalance during a start up of machinery. In Table 1, values of the fundamental natural frequency, mass and the critical damping ratio of the experimental structure are given. These values were measured when each oscillator was tested individually as a single-d.o.f. system. Structural parameters used in the numerical model (namely, the mass, damping coefficient and the stiffness) were calculated from the values reported in Table 1 for easy comparison with the experimental results described in the next section. The excitation frequency ω was changed linearly up to the tuning frequency, and kept constant at this frequency to represent the acceleration and the steady state. The constant C of the excitation is arbitrary, since the system equations are linear.

Displacement histories of the primary structure in Figure 6(a)–6(c) correspond to constant damping ratios of the absorber of 0.02, 0.05 and 0.20 as the frequency of excitation traverses from rest to the tuning frequency Hz in 100 s. Absorber's damping ratio of 0.02 corresponds to the case when the structure described in the Section 3 is used as the tuned absorber for the primary structure to be controlled, with full voltage applied across the ER fluid. Damping ratios of 0.05 and 0.20 are the two extreme values observed experimentally with a sloshing ER fluid (no voltage). Figure 6(d) and 6(e) correspond to the cases where the damping coefficient is kept at either 0.05 or 0.20, respectively, until 100 s, and then changed to 0.02. Histories of the displacement of the absorber in Figure 7(a)–7(e) correspond to the same cases in Figure 6. In order to fit in the same vertical scale, displacements in Figure 7(a), 7(b) and 7(d) were divided by 2.5 before plotting.

As expected from the frequency response in Figure 1(b), as the damping ratio of the tuned absorber increases, the peak displacement during transient resonance (around 84 s) decreases from 15 mm (with a ζ of 0.02) to approximately 5 mm (with a ζ of 0.20). In addition, as the damping ratio increases, the steady state displacement increases after 100 s from 0.4 mm (with a ζ of 0.02) to 3.5 mm (with a ζ of 0.20). As shown in Figure 6(d) and 6(e), when the damping ratio is varied at 100 s, corresponding to the case where the ER fluid is

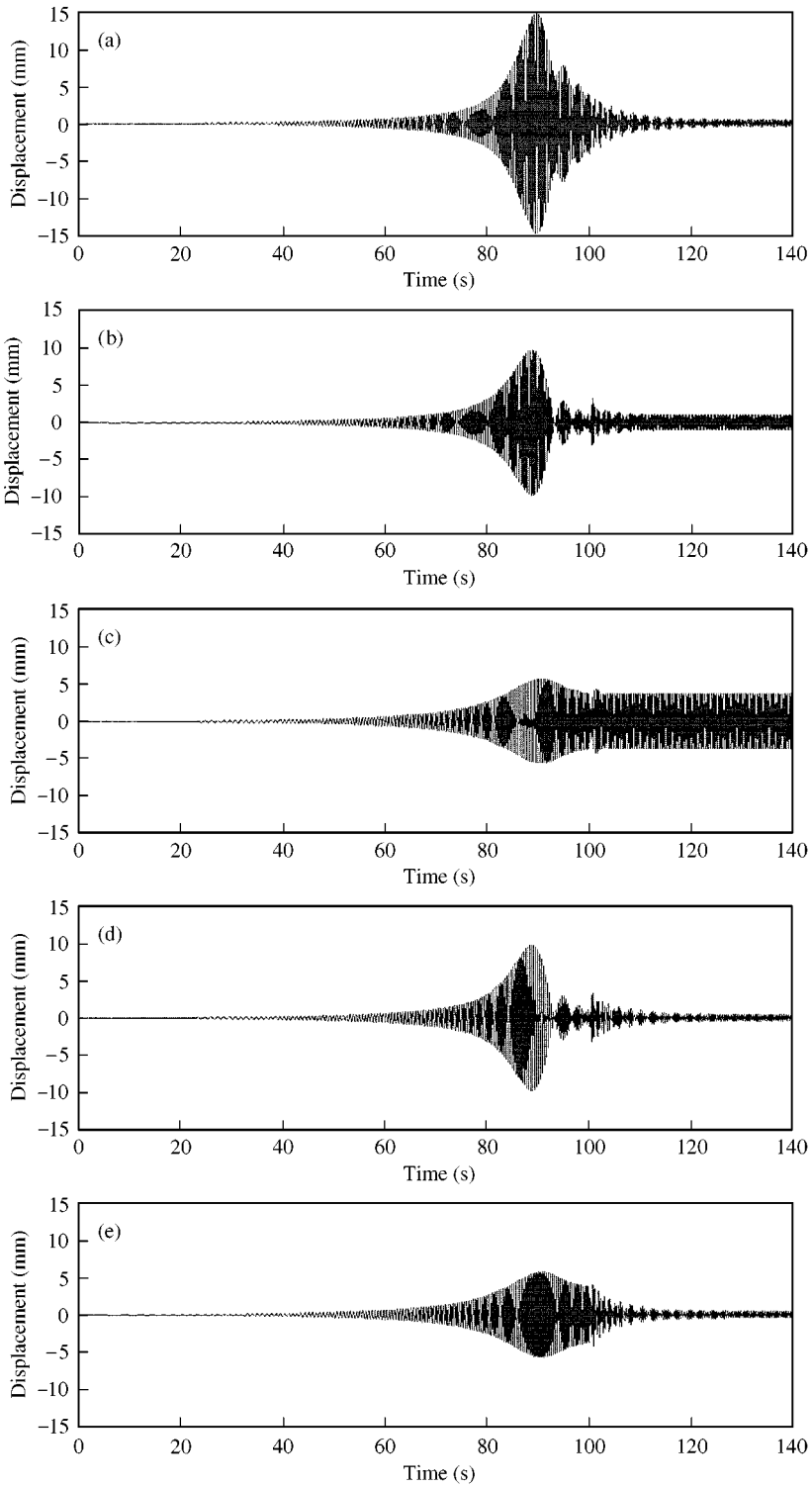


Figure 6. Displacement history of the primary structure with a constant ζ of (a) 0.02, (b) 0.05, (c) 0.20; and with a variable ζ of either (d) 0.05 or (e) 0.20 until 100 s and 0.02 after 100 s.

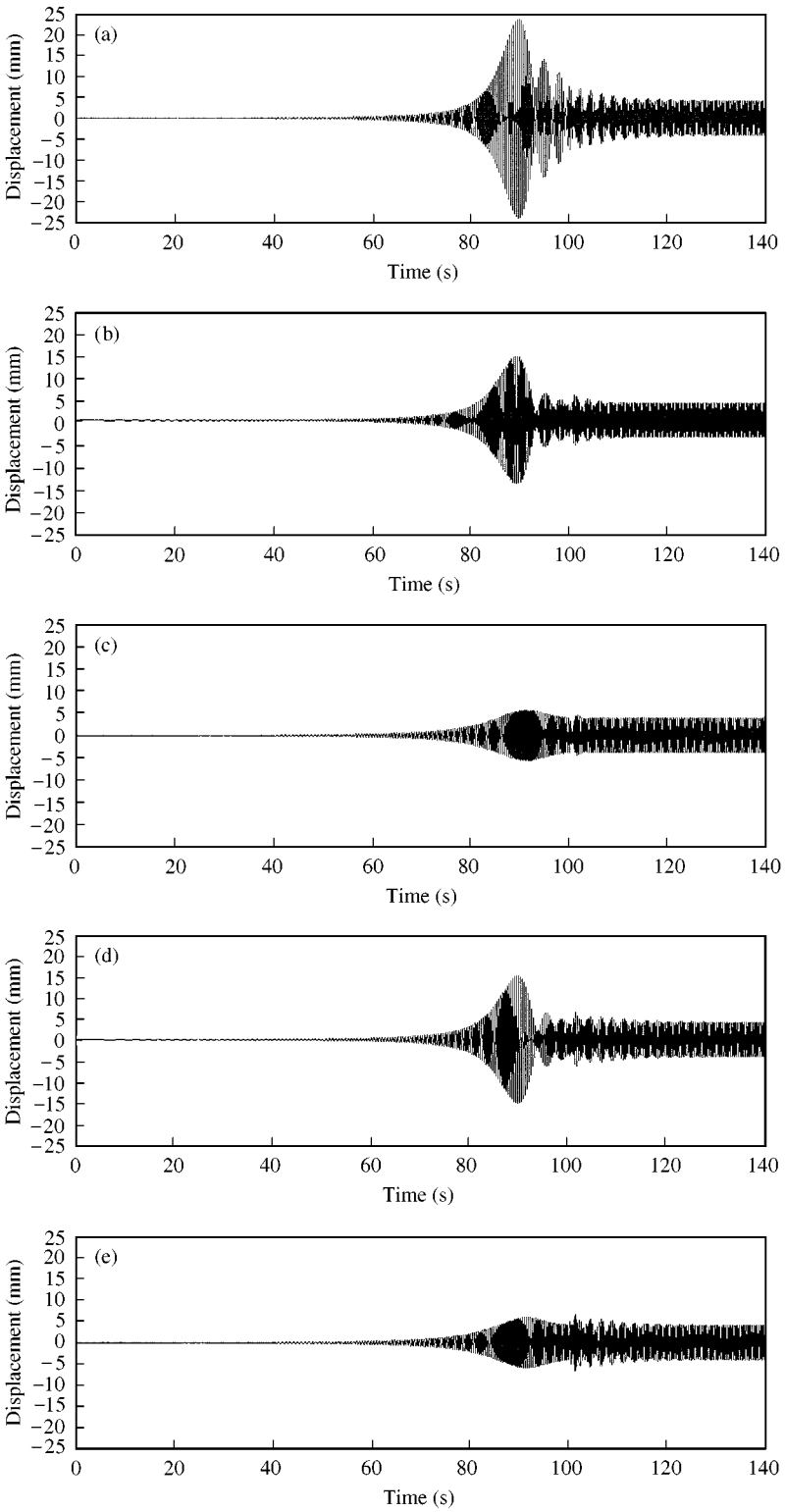


Figure 7. Same as in Figure 6, but for the tuned absorber.

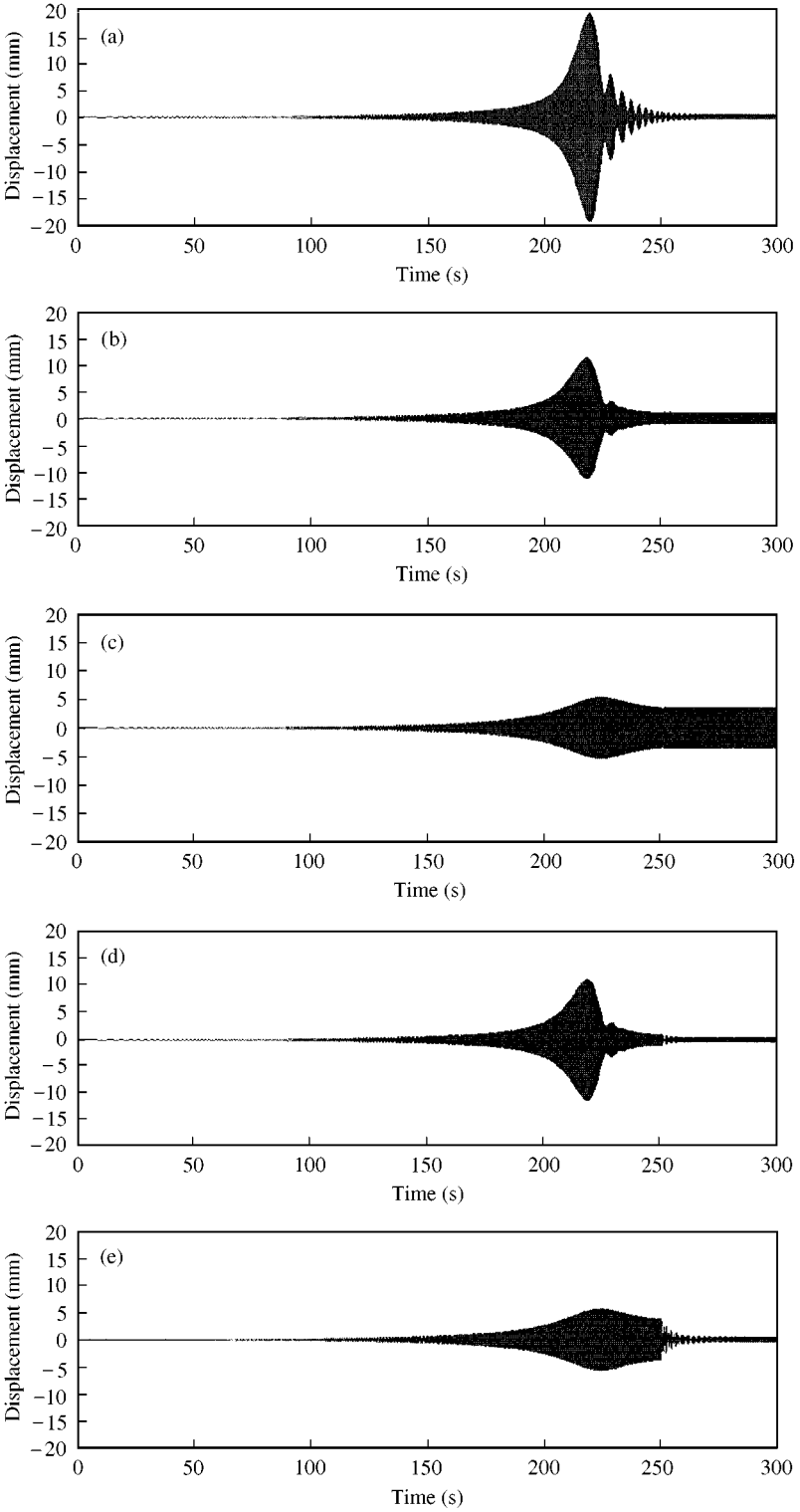


Figure 8. Same as in Figure 6, but for an acceleration over 250 s.

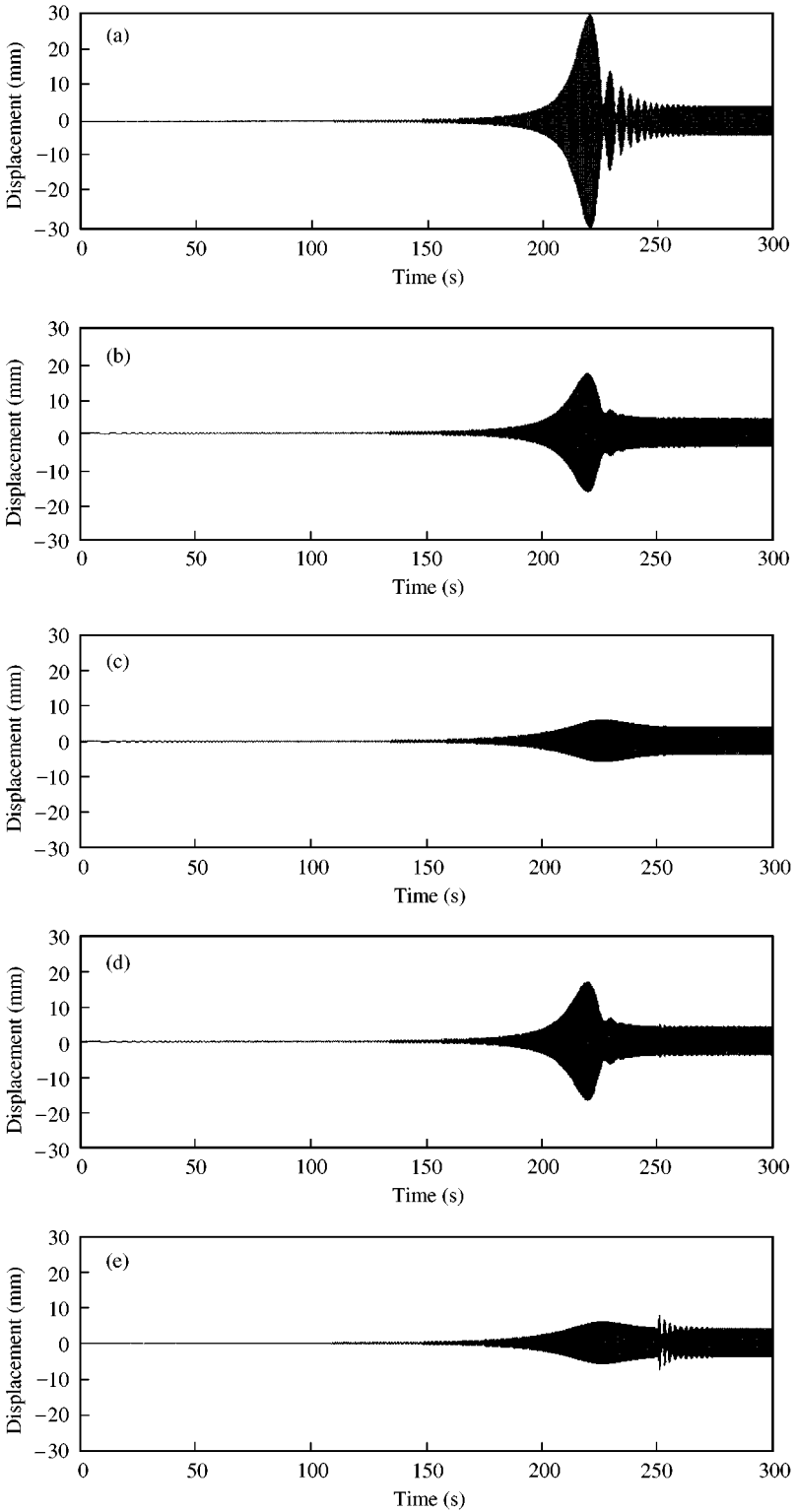


Figure 9. Same as in Figure 7, but for an acceleration over 250 s.

solidified, it is possible to retain the smaller response of high damping during acceleration, and that of the low damping during the steady state.

Figures 8 and 9 correspond to the displacement histories of the primary structure and the tuned absorber of the same damping coefficients as in Figures 6 and 7, but for a longer acceleration time of 250 s rather than 100 s (again, as in Figure 7, absorber displacements in Figure 9(a), 9(b) and 9(d) were divided by 2.5 to maintain a uniform vertical scale in Figure 9). This change in the acceleration time is important practically since a gradual acceleration would require less reserve power than a fast acceleration, and hence, resulting in a more economical designation of the power source. The price of a gradual acceleration, however, is that large resonance amplitudes are allowed to develop, as the first resonance frequency of the combined system is traversed slowly. This last trend is particularly true for light damping where the peak displacement grows to approximately 19 mm for ζ of 0.02, whereas it is still around 5 mm for ζ of 0.20, as shown in Figure 8(a) and 8(c) respectively. Therefore, being able to maintain high-damping during acceleration, and switching to low-damping in the steady state has even more critical importance for slow acceleration.

It should be mentioned here that the linear model employed in this section is not claimed to have a true representation of the rather complex energy dissipation characteristics which result from a sloshing liquid. The purpose of including this model is merely to demonstrate the effects of either the existence or the lack of energy dissipation during different phases of the problem.

5. EXPERIMENTS

Figure 10 shows the experimental set-up used to implement the suggested control with the sloshing ER fluid as the means to vary damping of a tuned absorber. The structure in Figure 5(a) is mounted on a similar mechanical oscillator made up of a rigid plate and four aluminium strips to represent the primary structure. Table 1 has the structural parameters of the system. Experimental procedure consisted of running a DC electric motor with a rotating unbalance disk (item 6) whose speed was controlled to vary linearly in 100 s. Acceleration times longer than 100 s could not be generated reliably with the available controller. The speed was kept constant at the tuning frequency for an additional 40 s to observe the steady state response. The response of the structure was measured with the same laser displacement transducer discussed earlier (shown mounted on the primary structure).

In Figure 11(a), the displacement history of the primary structure is shown with the full voltage on the ER fluid. This particular case displays the transient resonance very clearly around 90 s with a peak displacement response of approximately 11 mm. Steady state is reached around 110 s with a 1 mm peak response. The two smaller peaks around 50 and 70 s, indicate the resonances of the counterbalance weights of the rotating disk. The jump change towards the end marks a new transient when the electric motor is stopped.

The displacement history in Figure 11(b) corresponds to the freely sloshing ER fluid with no voltage applied on it. As a result of effective dissipation, the transient resonance is virtually non-existent, whereas the steady state displacement reaches as large as 7 mm around 100 s. In Figure 11(c), the variable damping case is shown where the ER fluid is allowed to slosh freely until 100 s, and solidified after 100 s. As expected, the smaller response of the two cases in Figures 11(a) and 11(b) are successfully combined in Figure 11(c).

The energy dissipation provided by the sloshing ER fluid, as shown in Figure 11(b), is quite different than what could be predicted with the linear viscous model in Figures 6 and 8. As discussed earlier in section 3, amount of energy dissipated with sloshing varies

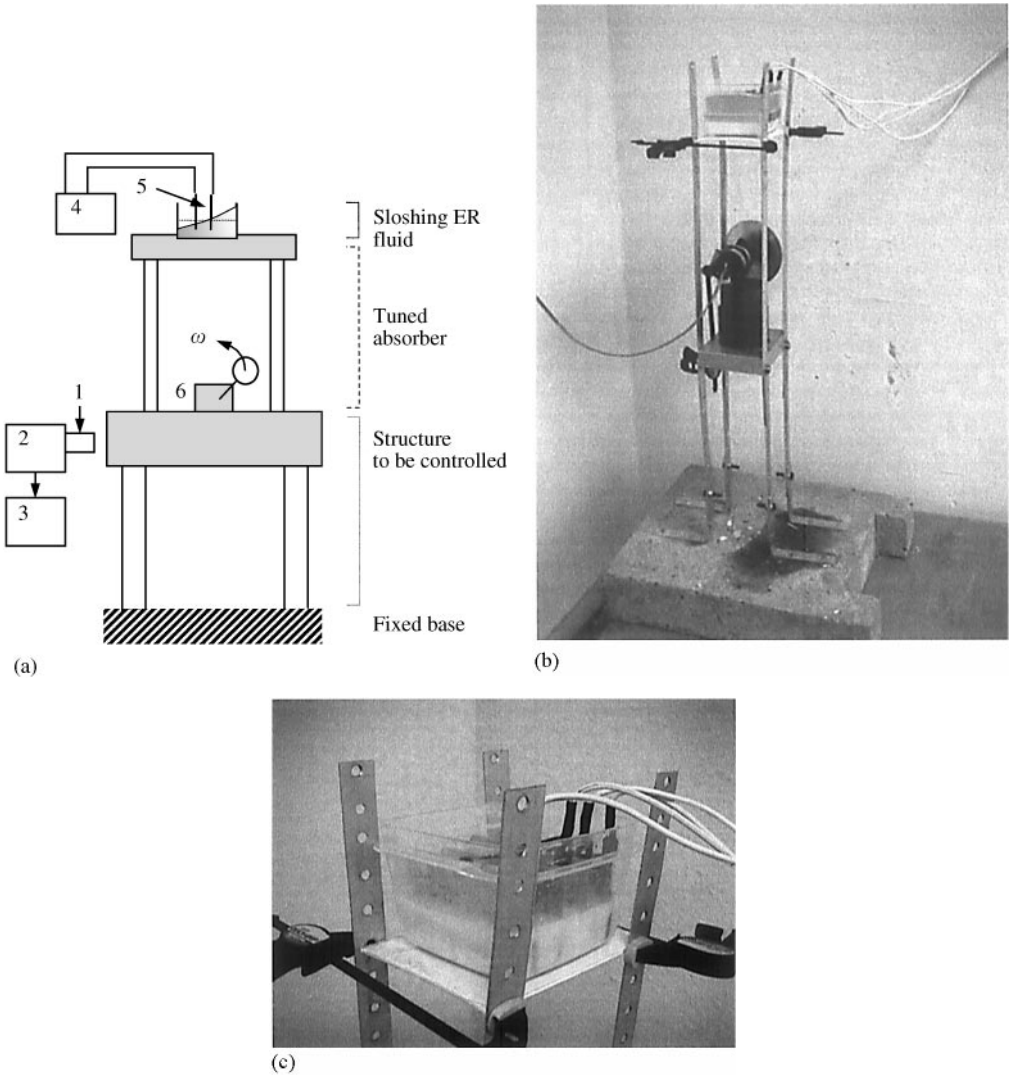


Figure 10. (a) Schematic of the experimental set-up where the experimental apparatus is the same as in Figure 5(a) with the addition of 6, Radio Spares — RS 266-985 DC electric motor with an unbalance disk, and photographs showing (b) the structure and (c) the detail of the sloshing container.

with the amount of shearing in the flow which is proportional to the amplitude of the sloshing wave. In Figure 12(a)–12(c), displacement history of the absorber is shown for the same three cases in Figure 11. Noise in Figure 12(a) is due to the saturation of the non-contact transducer for amplitudes larger than 20 mm. The history in Figure 12(b), corresponding to the freely sloshing ER fluid, suggests that the sloshing wave amplitude steadily grows from rest to the tuning frequency. This was verified visually during measurements. As the frequency of the excitation grows close to the first resonance frequency of the combined structure, the effective damping ratio also grows in concert with the growing wave amplitude. With increasing damping in the system, the resonance frequency is constantly pushed to a higher frequency such that the excitation can never catch up with it until the tuning frequency is reached. As a result, the highest rate of dissipation occurs in the steady state producing the large displacements of the primary structure.

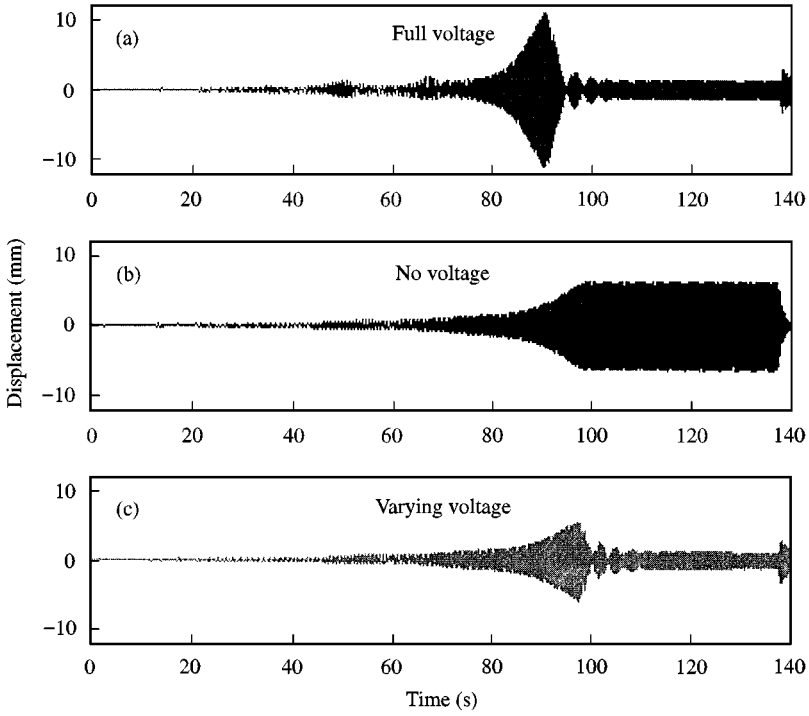


Figure 11. Experimentally observed displacement history of the primary structure with (a) full voltage, (b) no voltage and (c) no voltage until 100 s and then full voltage.

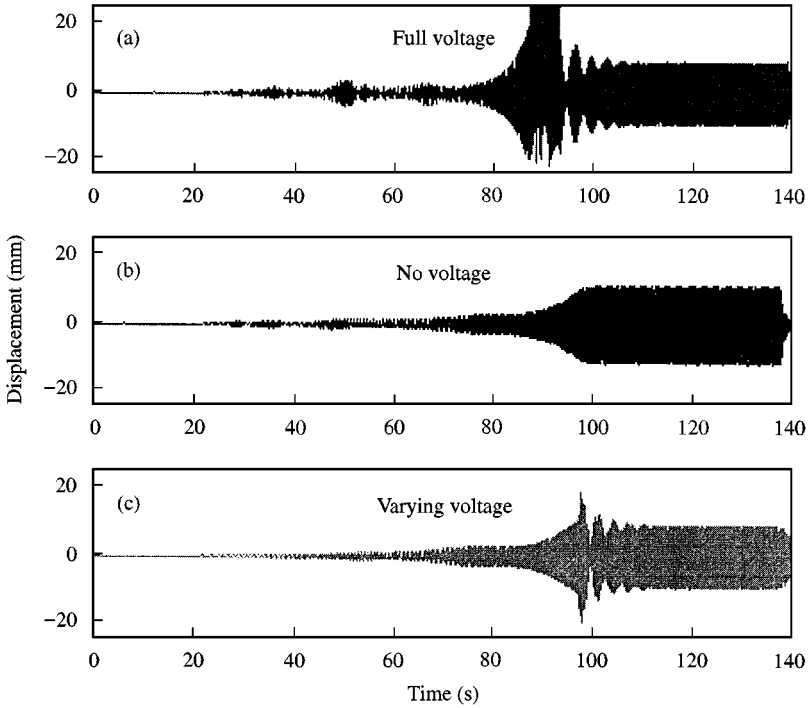


Figure 12. Same as in Figure 11, but for the tuned absorber.

6. CONCLUSIONS

ER fluids have the unique ability to change phase between liquid and a solid-like gel with the variation of the electrical potential across them. This phase change presents opportunities which could be exploited as an agent to switch the dissipation of energy of a tuned vibration absorber. The facility of varying damping is very useful when a tuned absorber has the task of suppressing both the resonant response in transient and the steady state response at the frequency of operation.

Simple numerical simulations presented in this paper indicated promise of the variable damping tuned absorber. Later, experiments demonstrated that it was possible to realise the benefits predicted by numerical simulations. However, differences occurred between the experimental observations and numerical predictions. It is believed that the differences arise due to the fact that sloshing is a non-linear phenomenon and this non-linearity causes the increase of the rate of dissipation with increasing wave amplitude. ER fluids hold potential in applications of vibration control.

ACKNOWLEDGMENTS

This project was financed by an infrastructure grant from The Victoria University of Technology. Dr Mark Hodge, of METSS Corporation, Columbus OH, U.S.A. and Dr Chris K. Mechefske, Department of Mechanical and Materials Engineering of the University of Western Ontario – Canada, were contributors in securing the grant.

REFERENCES

1. J. B. HUNT 1979 *Dynamic Vibration Absorbers*. Letchworth, London: The Garden City Limited.
2. J. C. SNOWDON 1968 *Vibration and Shock in Damped Mechanical Systems*. New York: John Wiley & Sons.
3. F. HARA and H. SHIBATA 1987 *Japanese Society of Mechanical Engineers International Journal* **30**, 318–323. Experimental study on active suppression by gas bubble injection for earthquake induced sloshing in tanks.
4. S. HAYAMA and M. IWABUCHI 1986 *Bulletin of Japanese Society of Mechanical Engineers* **29**, 1834–1841. A study on the suppression of sloshing in a liquid tank (1st Report, suppression of sloshing by means of a reversed U-tube).
5. K. MUTO, Y. KASAI and M. NAKAHARA 1988 *Transactions of the American Society of Mechanical Engineers, Journal of Fluids Engineering* **110**, 240–246. Experimental tests for suppression effects of water restraint plates on sloshing of a water pool.
6. J. G. ANDERSON, S. E. SEMERCIGIL and Ö. F. TURAN 2000 *Journal of Sound and Vibration* **232**, 839–856. A standing-wave-type sloshing absorber to control transient oscillations.
7. Y. GOUZZI, M. GUANG and F. TONG 1995 *Journal of Machine Vibration* **4**, 232–240. Electro-rheological fluid and its application in vibration control.
8. S. B. CHOI and Y. K. PARK 1994 *Journal of Sound and Vibration* **172**, 428–432. Active vibration control of a cantilevered beam containing an electro-rheological fluid.
9. T. TSUKIJI and N. TANAKA 1996 *American Society of Mechanical Engineers, Rheology and Fluid Mechanics of Nonlinear Materials*, AMD-Vol. 217. Effects of electrical change on the shear stress in ER fluid.
10. G. W. HOUSNER 1997 *Smart Material System* **123**, 937–943. Structural control: past, present and future.
11. D. M. ETTER 1993 *Engineering Problem Solving with Matlab*. NJ: Prentice-Hall Inc.